Supplementary Information

Zigzag Carbon as Highly Efficient and Stable Electrocatalyst for Oxygen Reduction Reaction in PEMFC

Xue et al.

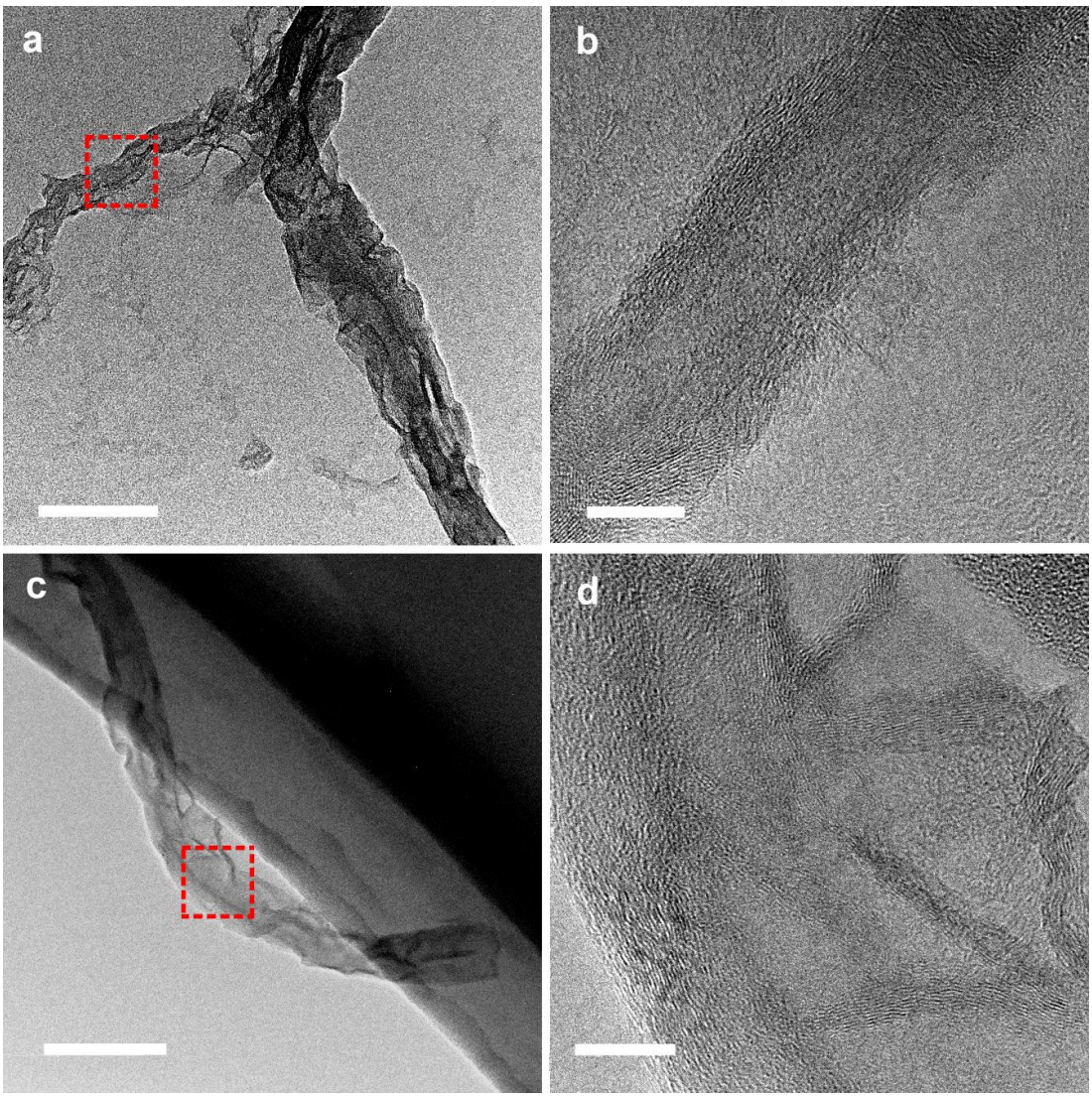

Supplementary Figure 1 | Morphologies of oxidized-GNR@CNT and oxidized-GNR before annealing. TEM images of (a-b) partially unzipped oxidized-GNR@CNT, and (c-d) fully unzipped oxidized-GNR. Scale bar in a, c is 100 nm, and in b, d is 10 nm.

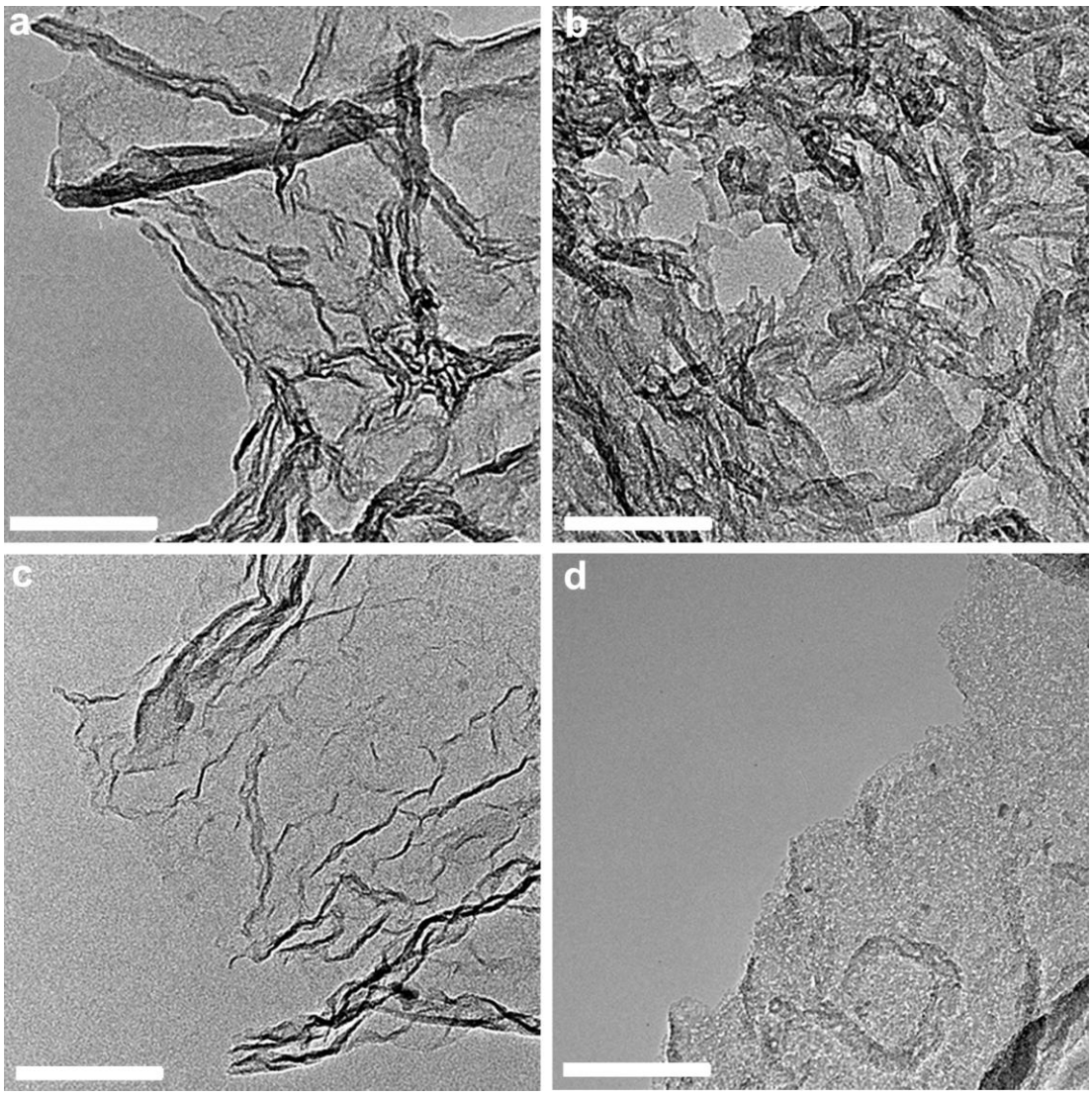

Supplementary Figure 2 | Morphologies of four samples after annealing. TEM images of (a) GNR@CNT, (b) N-GNR@CNT, (c) GNR and (d) N-GNR. Scale bar: 100 nm.

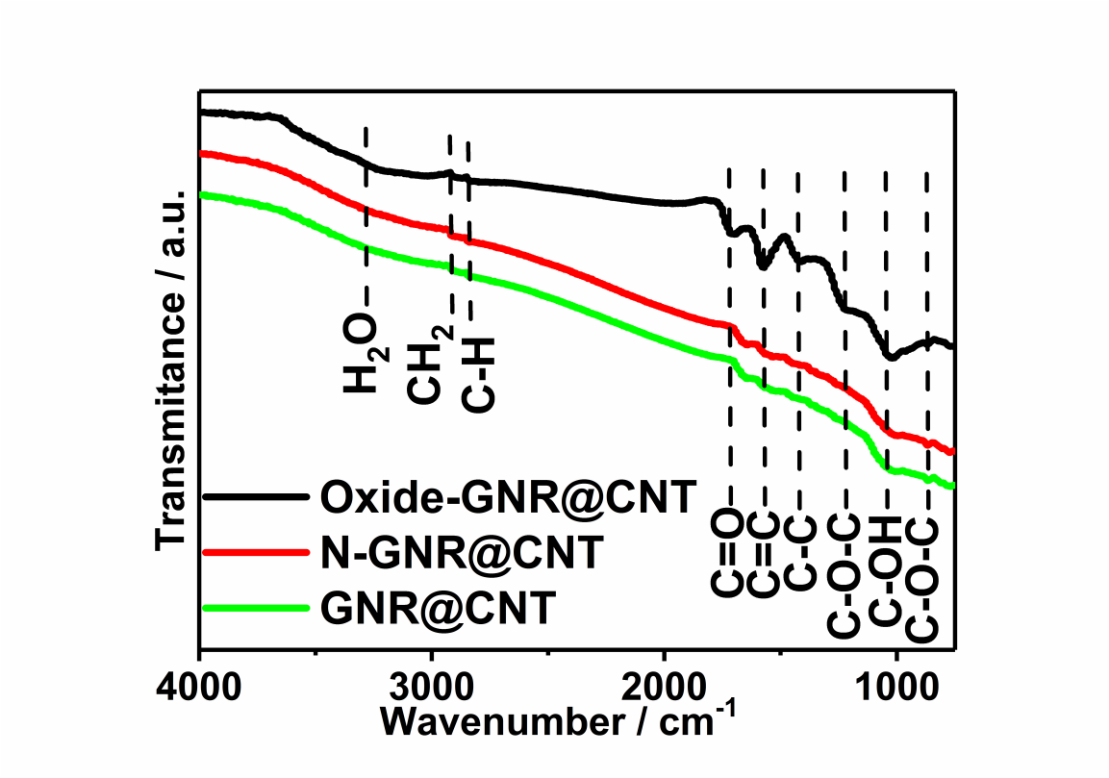

Supplementary Figure 3 | FT-IR spectra of Oxide-GNR@CNT, GNR@CNT and N-GNR@CNT.

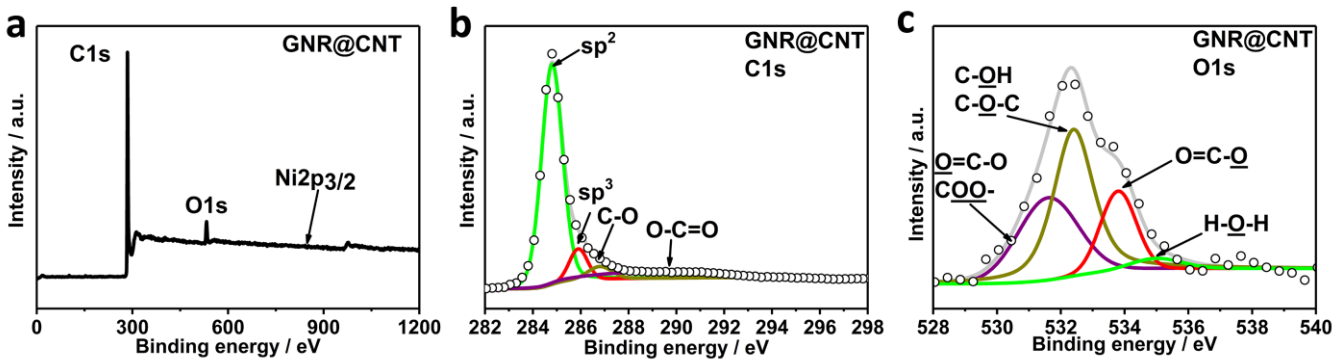

Supplementary Figure 4 | XPS spectra of GNR@CNT. (a) survey, and fine spectra of (b) C1s and (c) O1s.

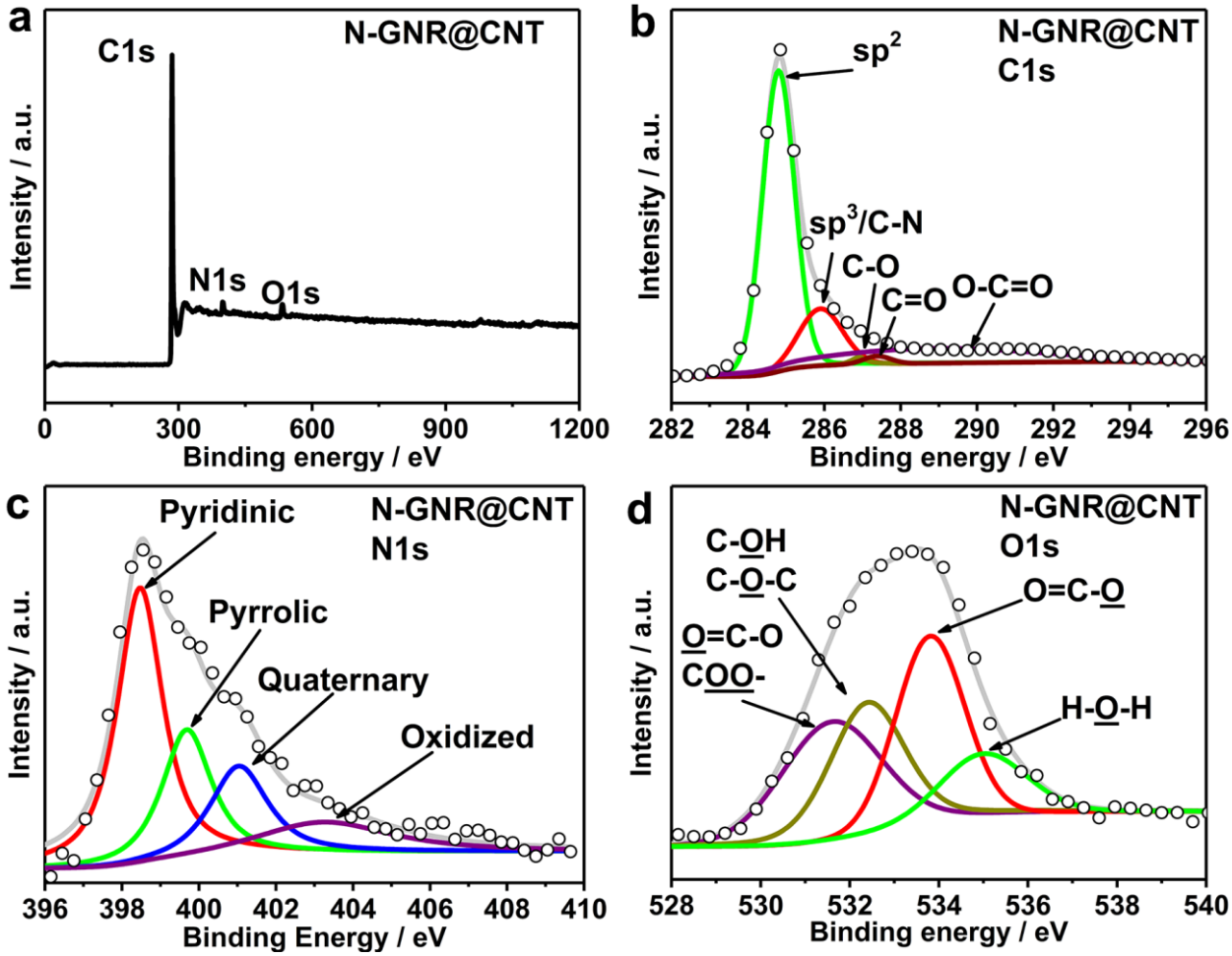

Supplementary Figure 5 | XPS spectra of N-GNR@CNT. (a) survey, and fine spectra of (b) C1s, (c) N1s and (d) O1s.

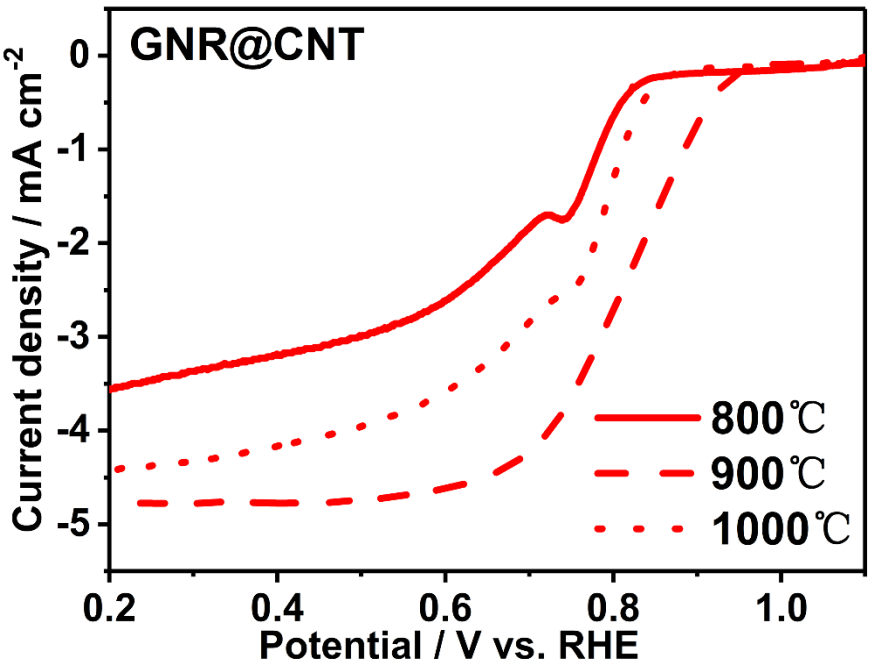

Supplementary Figure 6 | LSV curves of GNR@CNT annealed at different temperatures in Ar. The ORR were measured in O_2-saturated 0.1 M KOH at 1600 rpm. Scan rate: 10 mV s^{-1}.

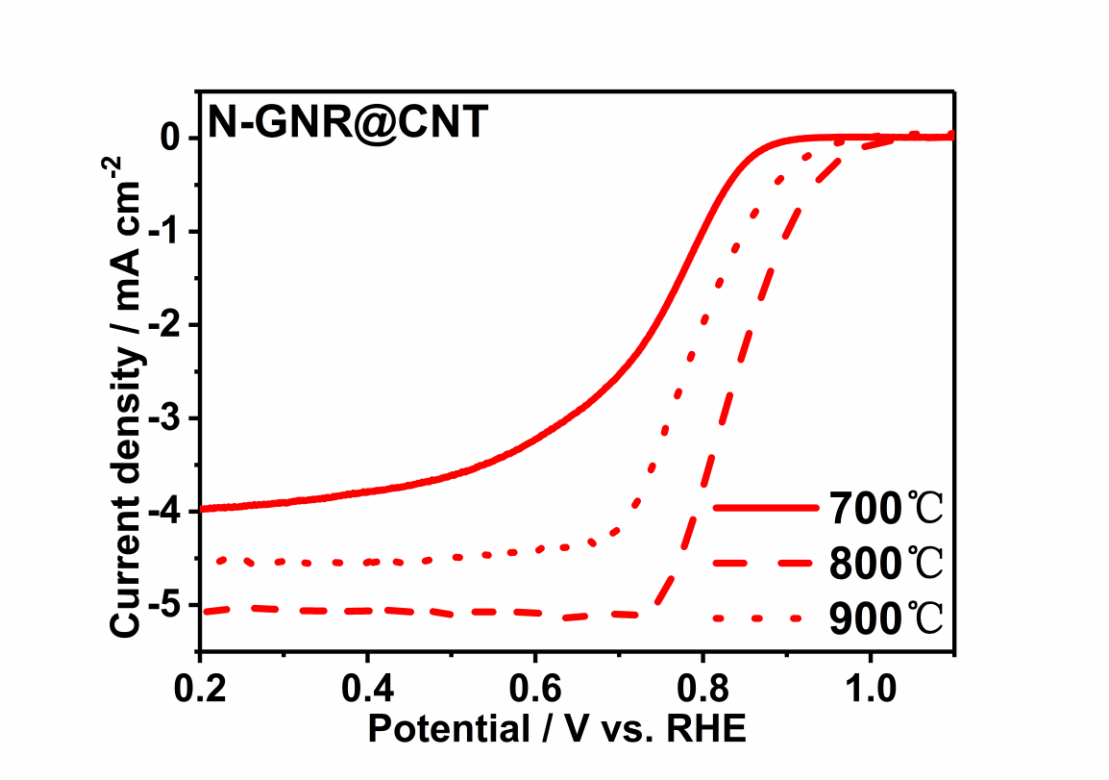

Supplementary Figure 7 | LSV curves of N-GNR@CNT annealed at different temperatures in NH_3.

The ORR were measured in O_2-saturated 0.1 M KOH at 1600 rpm. Scan rate: 10 mV s^{-1}.

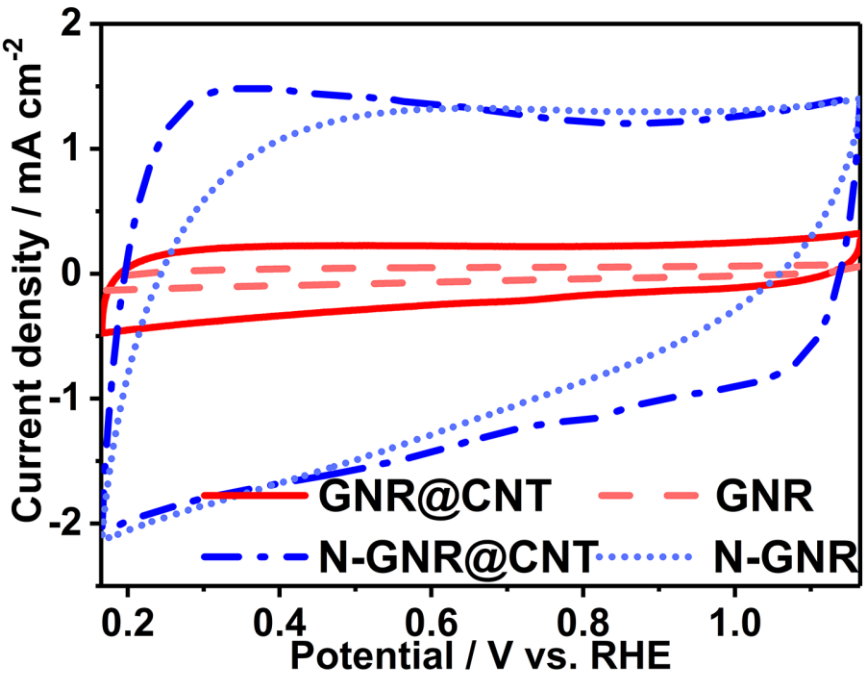

Supplementary Figure 8 | CV curves of four samples measured in N_2-saturated 0.1 M KOH. Scan rate: 50 mV s^{-1}.

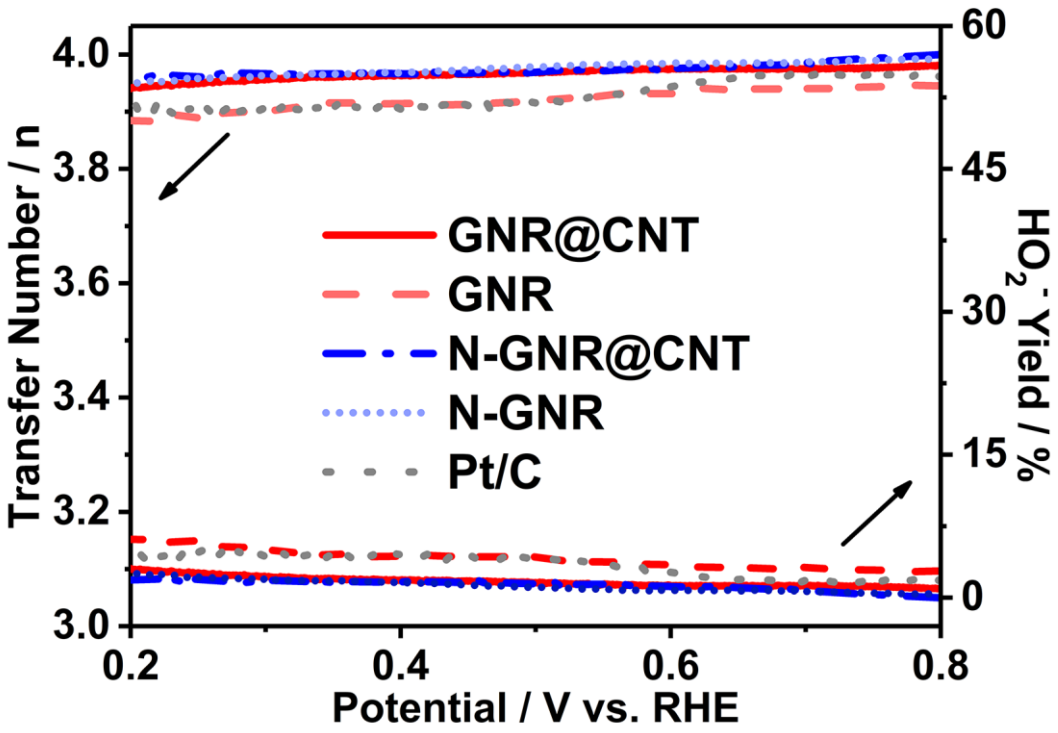

Supplementary Figure 9 | Electron transfer number and HO_2^- yield of GNR@CNT, GNR, N-GNR@CNT, N-GNR and Pt/C in O_2-saturated 0.1 M KOH at 1600 rpm. Scan rate: 10 mV s^{-1}.

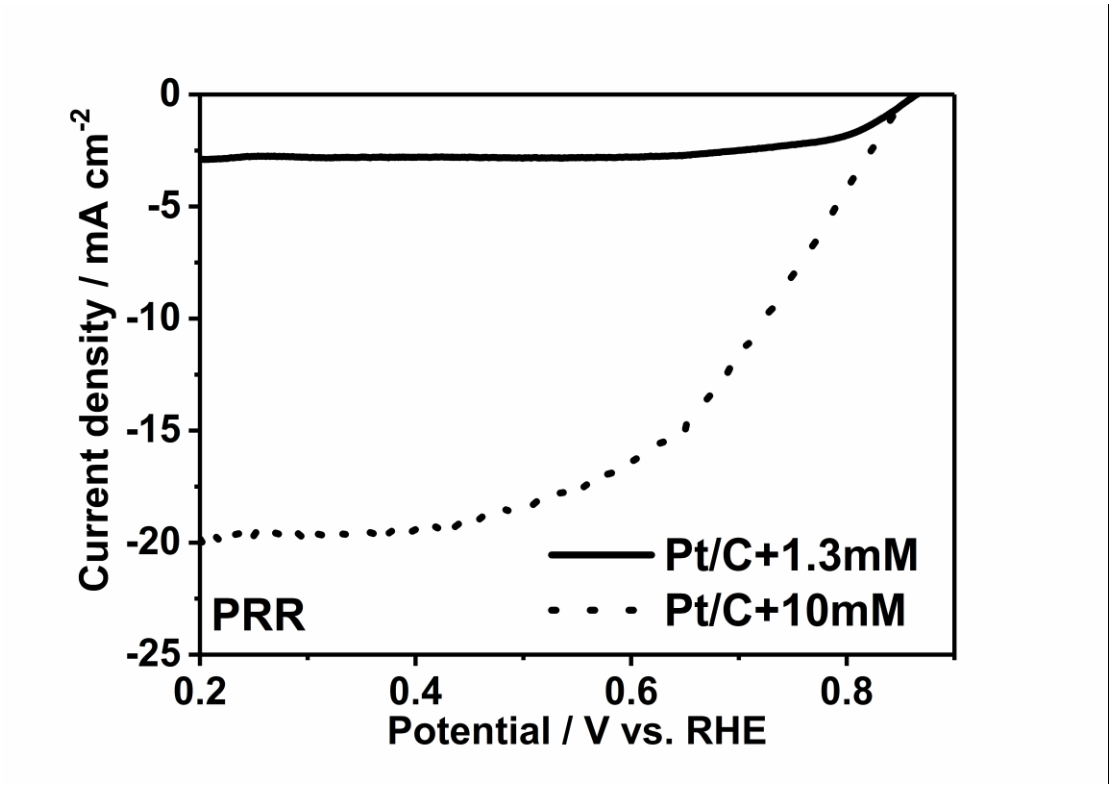

Supplementary Figure 10 | PRR polarization curves of Pt/C(20wt% Pt) measured in Ar-saturated 0.1 M KOH at 1600rpm. Scan rate: 10 mV s^{-1}.

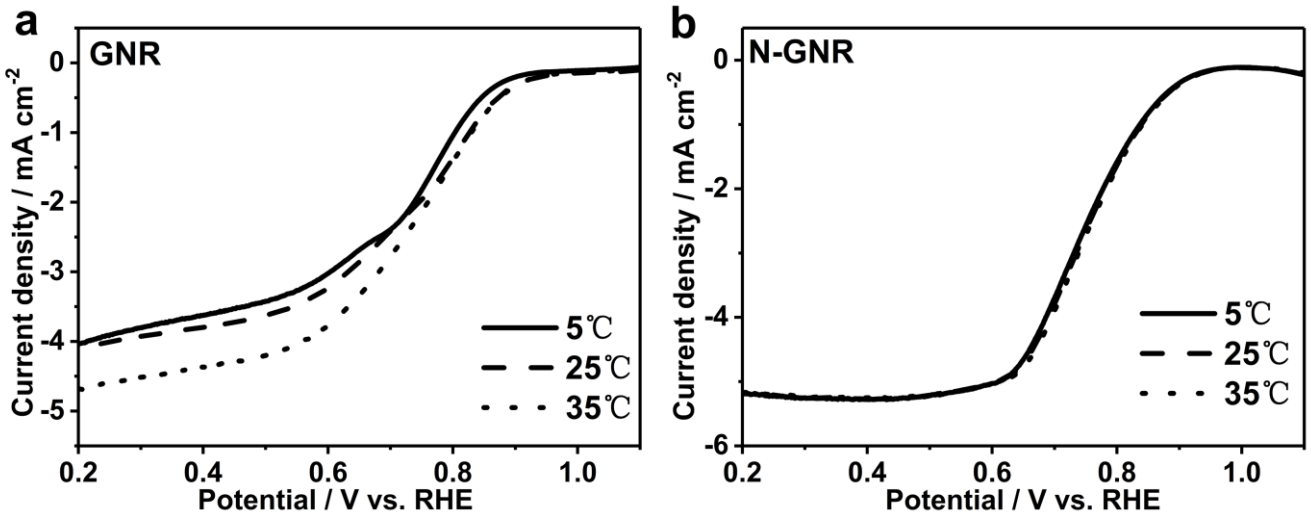

Supplementary Figure 11 | ORR responses to the testing temperature in alkaline. LSV curves of a) GNR and b) N-GNR measured at different temperatures in O_2-saturated 0.1 M KOH at 1600 rpm. Scan rate: 10 mV s^{-1}.

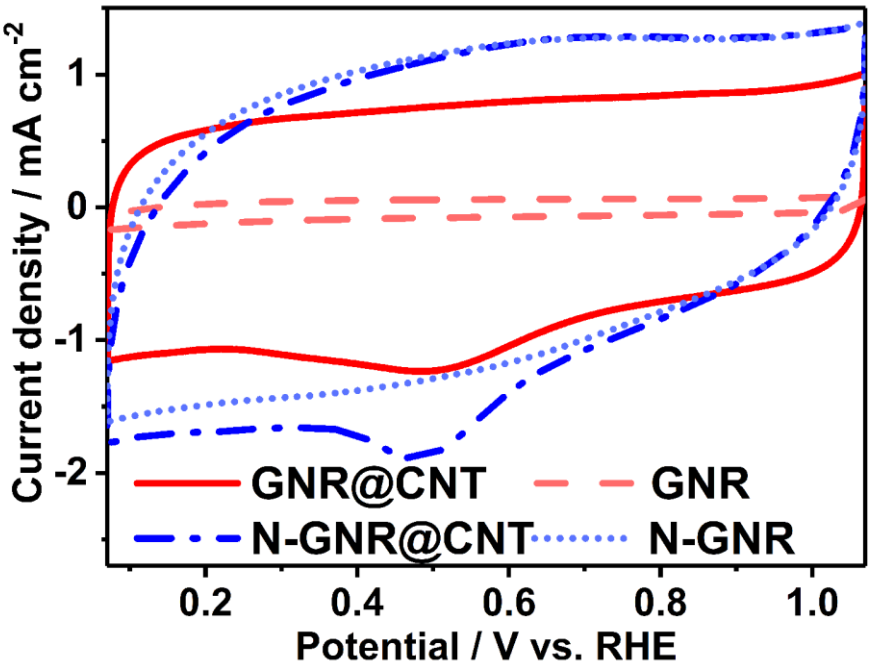

Supplementary Figure 12 | CV curves of indicated samples measured in N_2-saturated 0.5 M H_2SO_4. Scan rate: 50 mV s^{-1}.

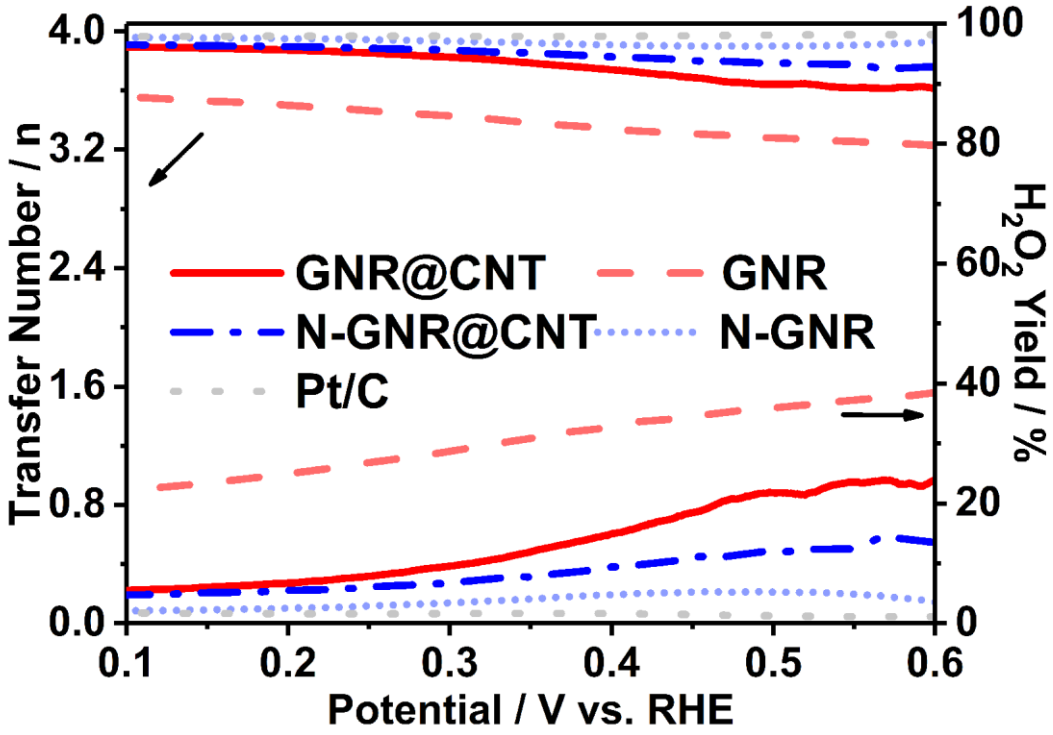

Supplementary Figure 13 | Electron transfer number and H_2O_2 yield of GNR@CNT, GNR, N-GNR@CNT, N-GNR and Pt/C in O_2-saturated 0.5 M H_2SO_4 at 1600 rpm. Scan rate: 10 mV s^{-1}.

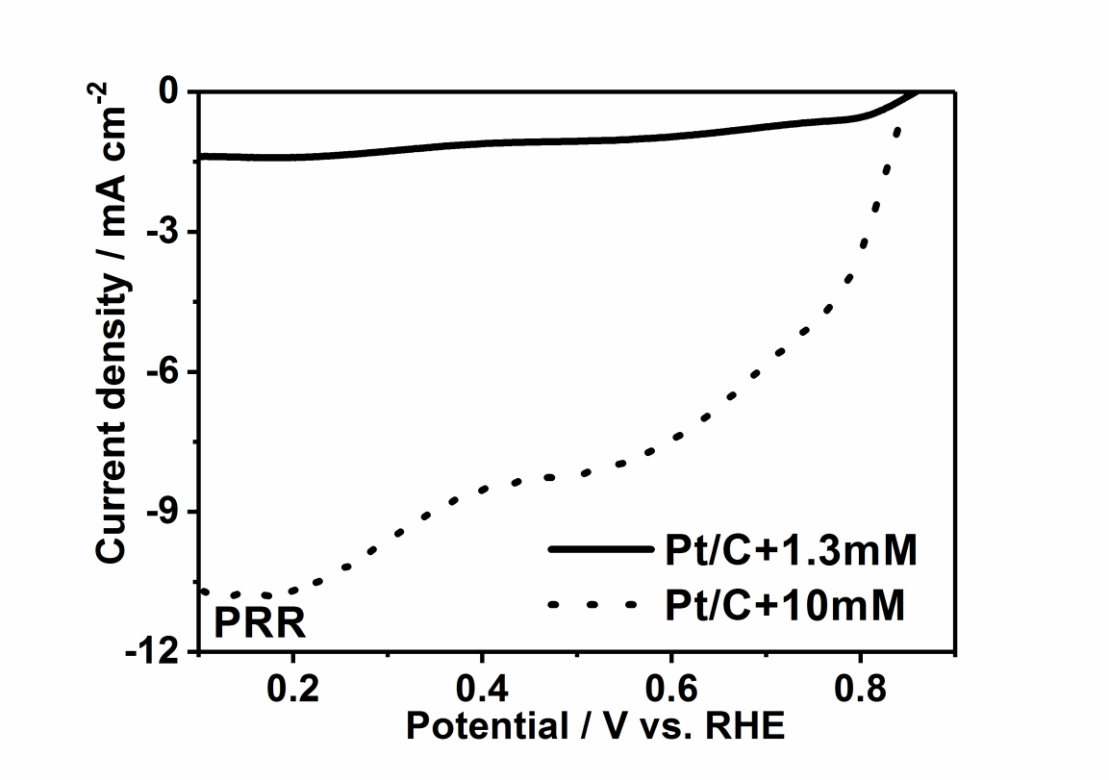

Supplementary Figure 14 | PRR polarization curves of Pt/C(20wt% Pt) measured in 0.5 M H_2SO_4 at 1600 rpm. Scan rate: 10 mV s^{-1}.

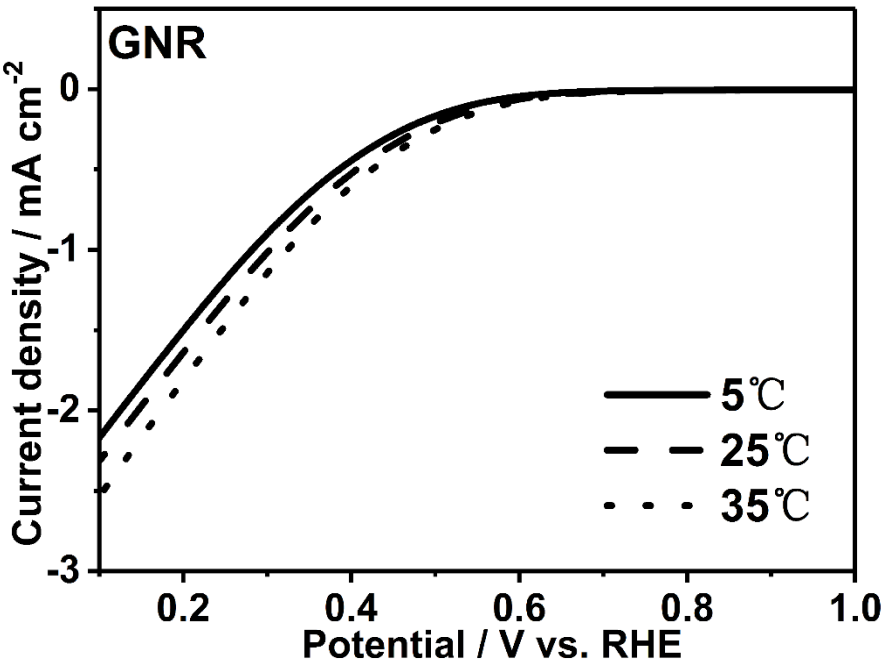

Supplementary Figure 15 | LSV curves of GNR measured at different temperatures in O_2-saturated 0.5 M H_2SO_4 at 1600 rpm. Scan rate: 10 mV s^{-1}.

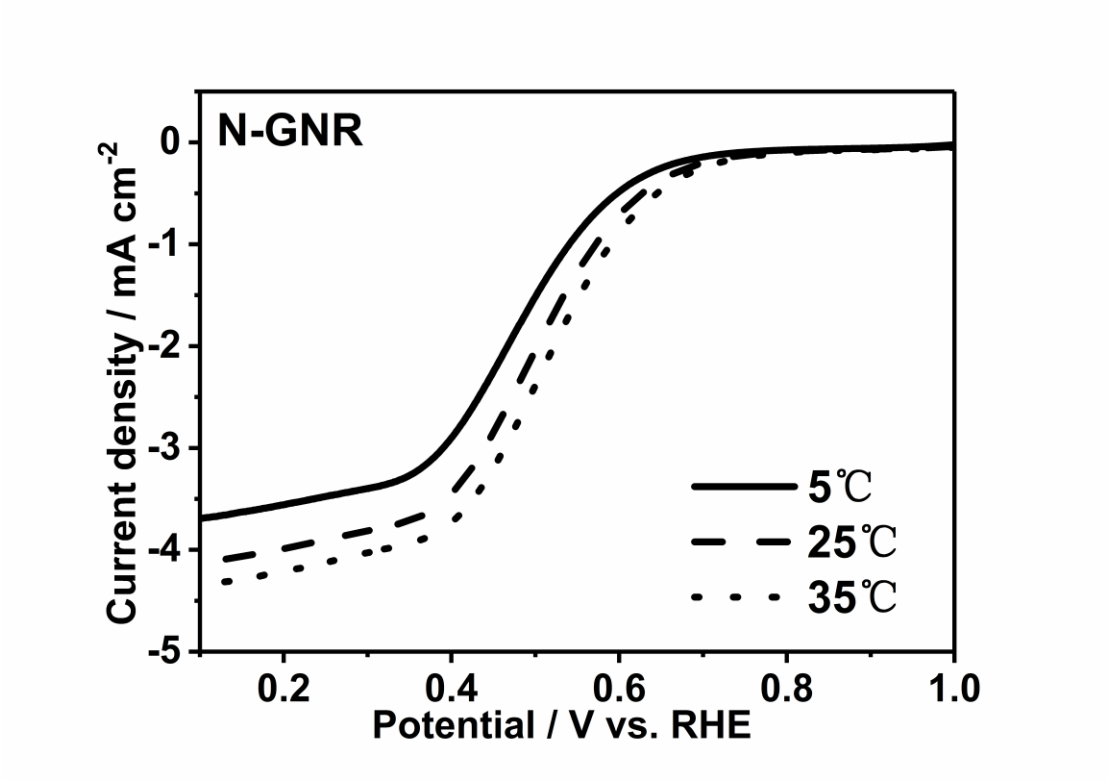

Supplementary Figure 16 | LSV curves of N-GNR measured at different temperatures in O_2-saturated 0.5 M H_2SO_4 at 1600 rpm. Scan rate: 10 mV s^{-1}.

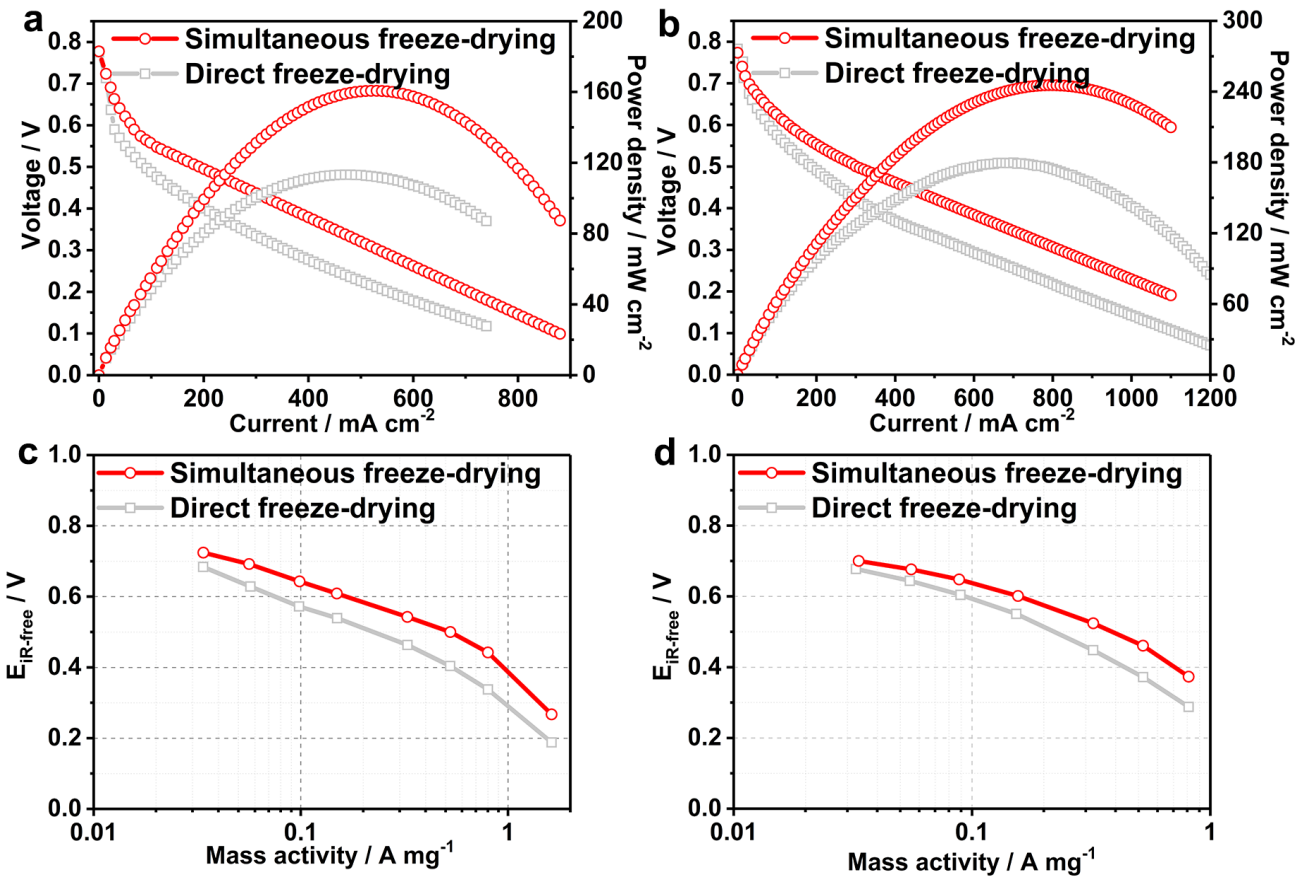

Supplementary Figure 17 | Polarization and power density curves of a) GNR@CNT+XC-72 (0.4+1.6 mg cm^{-2}) and b) N-GNR@CNT+XC-72 (0.9+2.2 mg cm^{-2}), and polarization curves expressed by $E_{iR\text{-}free}$ vs Log mass activity of c) GNR@CNT+XC-72 (0.4+1.6 mg cm^{-2}) and d) N-GNR@CNT+XC-72 (0.9+2.2 mg cm^{-2}) as cathode in PEMFC measured with 2 bar H_2–O_2, 100% RH, 80 °C.

Simultaneous freeze-drying: oxidized-GNR@CNT was mixed with XC-72 (spacer) first and then the mixture was freeze-dried and pyrolized. Direct freeze-drying: oxidized-GNR@CNT was freeze-dried and pyrolized to GNR@CNT or N-GNR@CNT first, and then they were mixed with XC-72 for catalyst ink. The PEMFC performance could be improved by enhancing the mass transfer of catalyst layer, through freeze-drying the catalyst precursor together with XC-72 before pyrolysis.

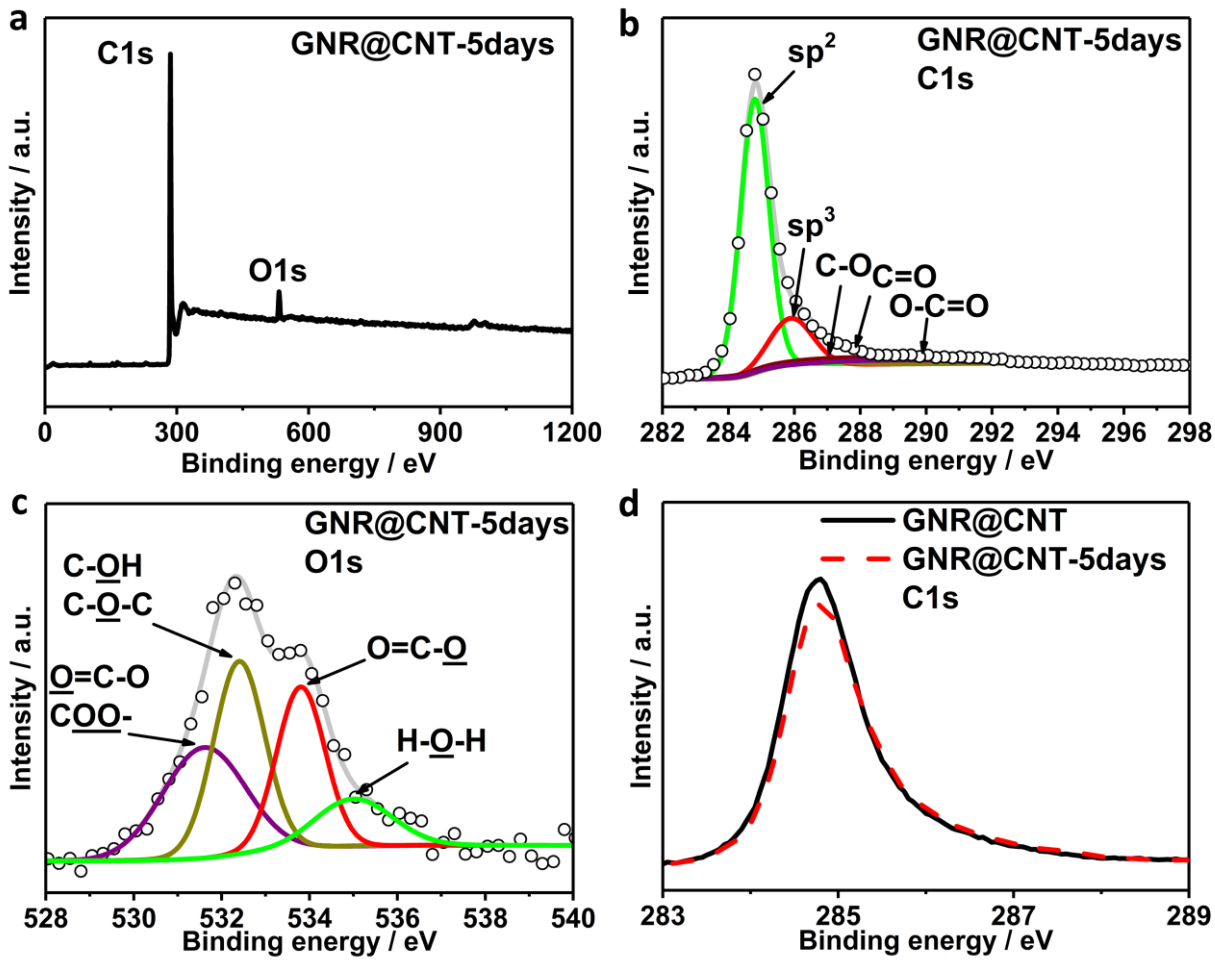

Supplementary Figure 18 | XPS spectra of GNR@CNT-5days. (a) survey, (b)C1s, (c) O1s and (d) a comparison of C1s spectra between GNR@CNT and GNR@CNT-5days.

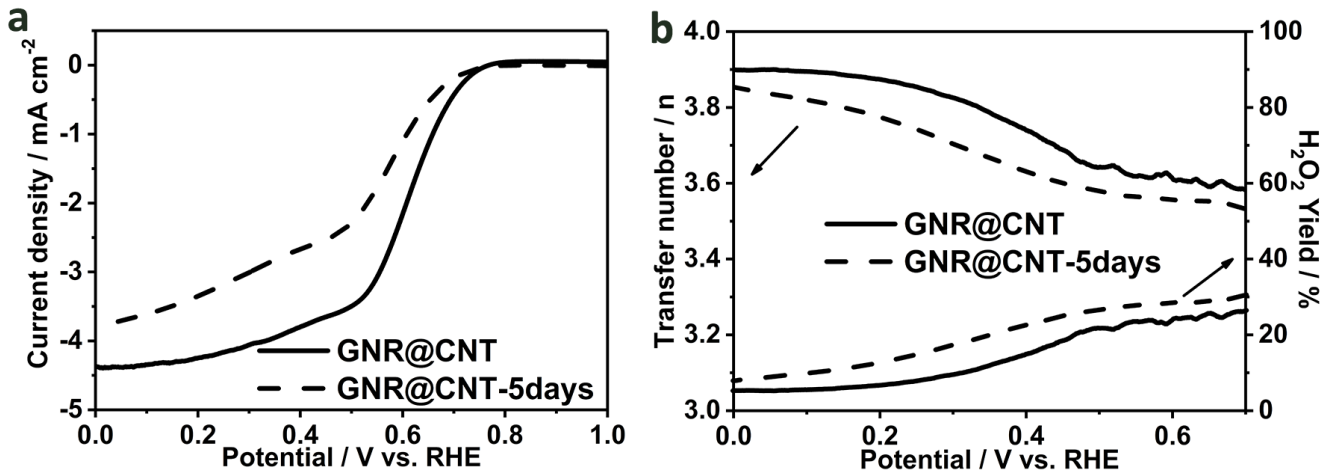

Supplementary Figure 19 | Half-cell performance comparison after air oxidization. (a) LSV curves and (b) electron transfer number and H_2O_2 yield of GNR@CNT (fresh) and GNR@CNT-5days (after exposed in air for 5 days) in O_2-saturated 0.5 M H_2SO_4 at 1600 rpm. Scan rate 10 mV s^{-1}.

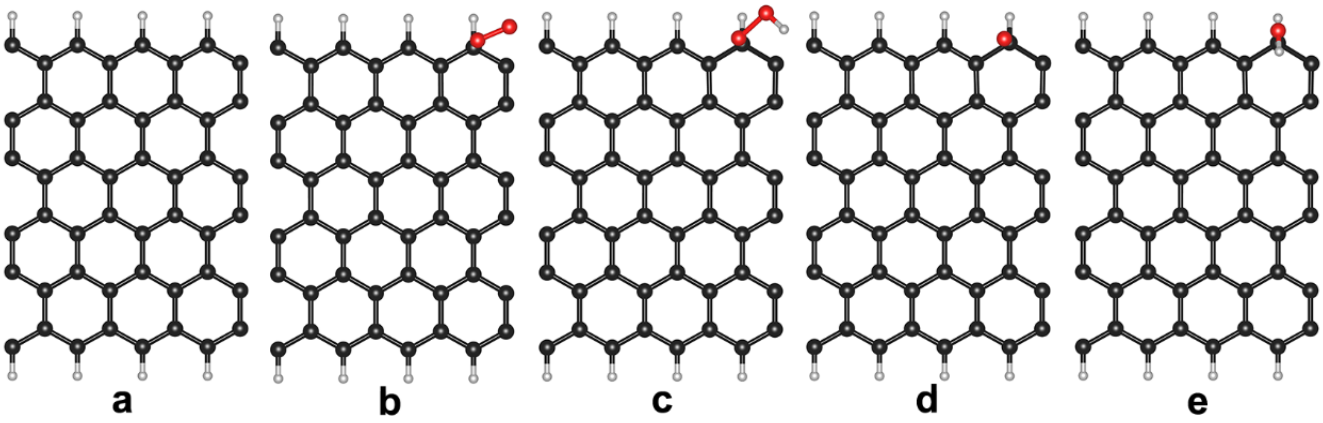

Supplementary Figure 20 | Schematic representation of ORR process on the zigzag-edge of graphene nanoribbon. (a) zigzag-edge graphene nanoribbons before ORR, (b) absorption of O_2 on a carbon at zigzag-edge, (c) adsorption of OOH after reaction with a proton, (d) adsorption of O after the release of a water molecule, and (e) adsorption of OH after reaction with a proton. Black, white, and red balls represent carbon, hydrogen, and oxygen atoms, respectively.

Supplementary Table 1 | Relative elemental contents of GNR@CNT, N-GNR@CNT and GNR@CNT-5days extracted from the XPS results

Samples	C1s [at.%]	sp^2/sp^3	N1s [at.%]	O 1s [at.%]				
				Total	COO- O=C-O	C-OH C-O-C	O=C-O	H-O-H
GNR@CNT	97.73	8.77	0	2.27	0.73	1.05	0.41	0.07
N-GNR@CNT	94.56	4.0[a]	3.09	2.35	--	--	--	--
GNR@CNT-5days	97.59	3.94	0	2.41	0.72	0.79	0.62	0.28

[a] C-N were contained in sp^3 for N-GNR@CNT.

Supplementary Table 2 | ORR activities of carbon-based metal-free electrocatalyst from literatures measured by half-cell in 0.1 M KOH.

Catalyst	Catalyst loading (mg cm^{-2})	Onset Potential (V vs. RHE)	Scan rate (mV s^{-1})	Rotation Rate (rpm)	Current Density at 0.4 V (mA cm^{-2})	Electron transfer number (n)	Reference
VA-NCNT	N.A.	0.976	5	1400	-3.90	3.9	[1]
CNT	0.255	0.846	10	1600	-2.1	3.1	[2]
N-porous carbon sheet	0.2	0.956	5	1600	-6.2	3.98	[2]
N-graphene	0.038	0.936	10	1600	-3.06	3.3	[3]
N-graphene/CNT	0.05	0.866	20	1600	-3	3.7	[4]
N-graphitic arrays	0.026	0.687	10	1600	-5.7	3.89	[5]
graphite-BM	0.1	0.816	10	1600	-1.75	3.8	[6]
CNC700	0.1	0.876	10	2500	-3.1	2.9	[7]
GNR	0.398	0.919	10	1600	-3.8	3.88	This work
N-GNR	0.398	0.946	10	1600	-5.2	3.95	This work
GNR@CNT	0.398	0.960	10	1600	-4.8	3.94	This work
N-GNR@CNT	0.398	0.990	10	1600	-5.1	3.96	This work

Supplementary Table 3 | ORR activities of carbon-based metal-free electrocatalysts from literatures (measured in acidic electrolytes).

Catalyst	Electrolyte	Catalyst loading (mg cm^{-2})	Onset Potential (V vs. RHE)	Scan rate (mV s^{-1})	Rotation Rate (rpm)	Current Density at 0.3 V (mA cm^{-2})	Electron transfer number (n)	Reference
N and P codoped mesoporous nanocarbon	0.1 M $HClO_4$	0.450	0.83	5	1600	4.70	3.8	[8]
N doped carbon nanotubes	0.5 M H_2SO_4	N.A.	0.70	10	1600	1.73	3.52-3.92	[9]
N doped carbon nanosheets	0.5 M H_2SO_4	0.600	0.72	10	1600	4.91	3.67-3.91	[10]
N doped carbon nanosheets	0.5 M H_2SO_4	0.051	0.725	20	1600	2.17	3.90-3.98	[11]
N doped mesoporous cabons	0.5 M H_2SO_4	0.312	0.720	10	1600	3.95	3.48	[12]
B and N codoped carbons	0.5 M H_2SO_4	0.200	0.57	10	1500	0.68	N.A.	[13]
GNR	0.5 M H_2SO_4	0.398	0.52	10	1600	1.02	3.19-3.59	This work
N-GNR	0.5 M H_2SO_4	0.398	0.68	10	1600	3.81	3.90-3.96	This work
GNR@CNT	0.5 M H_2SO_4	0.398	0.76	10	1600	4.06	3.61-3.90	This work
N-GNR@CNT	0.5 M H_2SO_4	0.398	0.75	10	1600	3.17	3.72-3.92	This work

Supplementary Table 4 | Gravimetric activities of various metal-free electrocatalysts compared with the N-GNR@CNT and GNR@CNT in PEM fuel cells. All the data in the table have also been scaled by the electrode surface area.

Materials	Current at 0.2 V (A g^{-1})	Peak power density (W g^{-1})	Catalyst loading (mg cm^{-2})	O_2-H_2 absolute pressure (bars)	Cell temperature (°C)	Reference
Co-PPY-C	725	156	0.8[a]	2.5	80	14
Fe/Phen/Z8	1500	233	3.9	1.5	N.A.	15
(CM+PANI)-Fe-C	900	225	4.0	2.5	80	16
20Co-NC-1100	N.A.	140	4.0	2.5	80	17
Fe2-Z8-C	N.A.	407	2.8	2.5	80	18
(Fe,Co)/N-C	N.A.	1272	0.77	2.5/1.5(O_2/H_2)	80	19
bNGr	N.A.	52	4	2.5	N.A.	20
DMWNT–H_2SO_4-Ar900	297	60	1.85	3.5	90	21
NG@MMT	750	160	2	N.A.	N.A.	22
VA-NCNT	1550	320	0.16	2.5	80	23
N-G-CNT+KB	1500	300	0.5	2.5	80	23
N-GNR@CNT+XC-72	2070/1950	420 / 380	0.25 / 0.5	2.5	80	This work
GNR@CNT+XC-72	2400/1153	520 / 235	0.25 / 0.5	2.5	80	This work

[a] Here we regard Co-PPY as catalyst and substrate the quality of carbon black.

Supplementary Table 5 | Open circuit voltage (OCV) of metal-free catalysts in PEMFC.

Materials	Catalyst loading / mg cm^{-2}	OCV / V_{RHE}
GNR	0.25	0.749
GNR@CNT		0.762
N-GNR		0.793
N-GNR@CNT		0.772
GNR	0.5	0.611
GNR@CNT		0.776
N-GNR		0.794
N-GNR@CNT		0.722

Supplementary references

1 Gong, K., Du, F., Xia, Z., Durstock, M. & Dai, L. Nitrogen-doped carbon nanotube arrays with high electrocatalytic activity for oxygen reduction. *Science* **323**, 760-764 (2009).

2 Zhong, H. X. *et al.* ZIF-8 derived graphene-based nitrogen-doped porous carbon sheets as highly efficient and durable oxygen reduction electrocatalysts. *Angew. Chem. Int. Ed.* **53**, 14235-14239 (2014).

3 Yang, S. *et al.* Efficient synthesis of heteroatom (N or S)-doped graphene based on ultrathin graphene oxide-porous silica sheets for oxygen reduction reactions. *Adv. Funct. Mater.* **22**, 3634-3640 (2012).

4 Chen, P., Xiao, T. Y., Qian, Y. H., Li, S. S. & Yu, S. H. A nitrogen-doped graphene/carbon nanotube nanocomposite with synergistically enhanced electrochemical activity. *Adv. Mater.* **25**, 3192-3196 (2013).

5 Liu, R., Wu, D., Feng, X. & Mullen, K. Nitrogen-doped ordered mesoporous graphitic arrays with high electrocatalytic activity for oxygen reduction. *Angew. Chem. Int. Ed.* **49**, 2565-2569 (2010).

6 Shen, A. *et al.* Oxygen reduction reaction in a droplet on graphite: direct evidence that the edge is more active than the basal plane. *Angew. Chem. Int. Ed.* **53**, 10804-10808 (2014).

7 Jiang, Y. *et al.* Significant contribution of intrinsic carbon defects to oxygen reduction activity. *ACS Catal.* **5**, 6707-6712 (2015).

8 Zhang, J., Zhao, Z., Xia, Z. & Dai, L. A metal-free bifunctional electrocatalyst for oxygen reduction and oxygen evolution reactions. *Nat. Nanotechnol.* **10**, 444-452 (2015).

9 Yu, D., Zhang, Q. & Dai, L. Highly efficient metal-free growth of nitrogen-doped single-walled carbon nanotubes on plasma-etched substrates for oxygen reduction. *J. Am. Chem. Soc.* **132**, 15127-15129 (2010).

10 Wei, W. *et al.* Nitrogen-doped carbon nanosheets with size-defined mesopores as highly efficient metal-free catalyst for the oxygen reduction reaction. *Angew. Chem. Int. Ed.* **53**, 1570-1574 (2014).

11 Chen, P. *et al.* Nitrogen-doped nanoporous carbon nanosheets derived from plant biomass: an efficient catalyst for oxygen reduction reaction. *Energy Environ. Sci.* **7**, 4095-4103 (2014).

12 Wang, X. *et al.* Ammonia-treated ordered mesoporous carbons as catalytic materials for oxygen reduction reaction. *Chem. Mater.* **22**, 2178-2180 (2010).

13 Ozaki, J.-I., Kimura, N., Anahara, T. & Oya, A. Preparation and oxygen reduction activity of BN-doped carbons. *Carbon* **45**, 1847-1853 (2007).

14 Bashyam, R. & Zelenay, P. A class of non-precious metal composite catalysts for fuel cells. *Nature* **443**, 63-66 (2006).

15 Proietti, E. *et al.* Iron-based cathode catalyst with enhanced power density in polymer electrolyte membrane fuel cells. *Nat. Commun.* **2**, 416 (2011).

16 Chung, H. T. *et al.* Direct atomic-level insight into the active sites of a high-performance PGM-free ORR catalyst. *Science* **357**, 479-484 (2017).

17 Wang, X. X. *et al.* Nitrogen-coordinated single cobalt atom catalysts for oxygen reduction in proton exchange membrane fuel cells. *Adv. Mater.* **30**, 1706758 (2018).

18 Liu, Q., Liu, X., Zheng, L. & Shui, J. The solid-phase synthesis of an Fe-N-C electrocatalyst for high-power proton-exchange membrane fuel cells. *Angew. Chem. Int. Ed.* **57**, 1204-1208 (2018).

19 Wang, J. *et al.* Design of N-coordinated dual-metal sites: a stable and active Pt-free catalyst for acidic oxygen reduction reaction. *J. Am. Chem. Soc.* **139**, 17281-17284 (2017).

20 Choi, C. H. *et al.* Long-range electron transfer over graphene-based catalyst for high-performing oxygen reduction reactions: importance of size, N-doping, and metallic impurities. *J. Am. Chem. Soc.* **136**, 9070-9077 (2014).

21 Waki, K. *et al.* Non-nitrogen doped and non-metal oxygen reduction electrocatalysts based on carbon nanotubes: mechanism and origin of ORR activity. *Energy Environ. Sci.* **7**, 1950-1958 (2014).

22 Ding, W. *et al.* Space-confinement-induced synthesis of pyridinic- and pyrrolic-nitrogen-doped graphene for the catalysis of oxygen reduction. *Angew. Chem. Int. Ed.* **52**, 11755-11759 (2013).

23 Shui, J., Wang, M., Du, F. & Dai, L. N-doped carbon nanomaterials are durable catalysts for oxygen reduction reaction in acidic fuel cells. *Sci. Adv.* **1**, e1400129 (2015).